ISSN (Print) 1226-1750
ISSN (Online) 2233-6656
Journal of Magnetics 23(3), 381-385 (2018) https://doi.org/10.4283/JMAG.2018.23.3.381

Improvement of Magnetic Properties of $SmCo_5/\alpha$-Fe Nanocomposite Magnets by Magnetic Field Annealing

Y. Wei, Y. Q. Li, D. T. Zhang, and M. Yue*

College of Materials Science and Engineering, Beijing University of Technology, Beijing, 100124, China

(Received 15 December 2017, Received in final form 12 August 2018, Accepted 20 August 2018)

In this paper, magnetic field heat treatment was carried out for the $SmCo_5/\alpha$-Fe amorphous powders prepared by high-energy ball milling. The effects of annealing temperature and magnetic field on the crystallization, microstructure, and magnetic properties of the $SmCo_5/\alpha$-Fe nanocomposite permanent magnets were studied. The results show that the magnetic field can benefit the crystallization of $SmCo_5$ phase and the degree of crystallinity of $SmCo_5/\alpha$-Fe alloy. Thus, the remanence and coercivity of the $SmCo_5/\alpha$-Fe magnets annealed with magnetic field are significant higher than those of the samples annealed without magnetic field. With the increase of annealing temperature in magnetic field heat treatment, the Sm(Co, Fe)$_5$ phase and FeCo phase are gradually crystallized and grew up, while a small amount of Sm_2Co_{17} phase appears. The best magnetic properties are M_r = 73.29 emu/g, M_r/M_s = 0.59, and H_{ci} = 6.20 kOe, when the annealing temperature is 700 ^oC.

Keywords : magnetic field heat treatment, $SmCo_5/\alpha$-Fe nanocomposite magnet, crystallization

Introduction

$SmCo_5$ permanent magnet is widely concerned because of its high magnetocrystalline anisotropy and Curie temperature. But the application of the magnet is limited for its low saturation magnetization and high raw material price. In recent years, nanocomposite magnets can provide an effective way for the SmCo-based permanent magnet to improve the saturation magnetization and reduce the cost of materials [1-9].

Recently, the research of $SmCo_5/\alpha$-Fe nanocomposite system has made great progress in permanent magnetic films. Neu et al. prepared the $SmCo_5/\alpha$-Fe nanocomposite films bearing the magnetic energy product of 50 MGOe, which is much larger than the theoretical magnetic energy product (32.5 MGOe) of single phase $SmCo_5$ magnet [10]. However, the coercivity of the $SmCo_5/\alpha$-Fe nanocomposite films is greatly reduced for the addition of the soft magnetic phase layer. The results show that excellent $(BH)_{max}$ is acquired for the $SmCo_5/\alpha$-Fe magnetic multilayers. However, it is still difficult for bulk $SmCo_5/\alpha$-Fe nanocomposite magnets to obtain such high magnetic properties. Traditional preparation methods are difficult to obtain bulk nanostructured magnets with ideal morphology, because high temperature will lead to excessive growth of grains thus damaging the exchange coupling and destroying the magnetic properties [11]. Therefore, much researches [12-16] have focused on new process to prepare bulk $SmCo_5/\alpha$-Fe nanocomposite magnets with ideal microstructure and excellent magnetic properties. Zhang *et al.* report the bulk SmCo/FeCo nanocomposite magnets with the $(BH)_{max}$ of 28 MGOe by combining temperature gradient, high pressure, and high stress thermal deformation techniques [17]. In addition, magnetic field annealing has been widely used in the preparation of magnetic materials as a new method of non-traditional heat treatment [18]. During heat treatment, the magnetic field can promotes the crystallization of the amorphous powders, allowing the phase transition at a lower temperature. At the same time, under the Curie temperature, the magnetic field can rearrange atoms in a very small local area so that the material has a preferential orientation along the magnetic field direction, resulting in induced anisotropy [19]. In 2004, Lian *et al.* study the effects of magnetic field heat treatment on the microstructure and magnetic properties of $Nd_{10.5}Fe_{76.4}Co_5Zr_2B_{6.1}$ permanent magnet [20]. The results show that the magnetic field can reduce the crystallization temperature and shorten the crystallization time of the amorphous Nd-Fe-B powder. Besides, the magnetic field heat treatment can also refine

*Corresponding author: Tel: +8615210377922
Fax: +010-67391760, e-mail: magnetic@bjut.edu.cn

the grain, enhance the intergranular magnetic exchange coupling effect and improve the magnetic properties. For Sm-Co-Fe amorphous alloy, the crystallization temperature is much lower than the Curie temperature. Thus, the magnetic field can mainly affect the crystallization process of Sm-Co-Fe alloy, thereby optimizing microstructure [21].

In this paper, $SmCo_5$/α-Fe amorphous powders are prepared by means of rapid quenching and high-energy ball milling. Magnetic field heat treatment is used during the crystallization of the $SmCo_5$/α-Fe. The effects of annealing temperature and magnetic field on the structure and magnetic properties of the $SmCo_5$/α-Fe nanocomposite magnet are studied systematically.

2. Experiment

The $SmCo_5$ + 20 wt.% α-Fe alloy ingot was prepared by induction melting with 5 wt.% excess of Sm to compensate for the evaporation losses. Then, the Sm-Co-Fe alloy ingot was manually crushed into powders with the size less than 125 μm. The crushed powders were milled for 10 h in a high energy ball mill under Ar. The ball-to-powder weight ratio was 20:1. The as-milled Sm-Co-Fe powders were put into a WC-Co mold and pressed into block samples under 500 MPa at room temperature.

The samples were annealed at 400 °C-800 °C for 2 h in a vacuum furnace with a parallel stable magnetic field of 3 T. The schematic diagram of magnetic field heat treatment was shown in Fig. 1.

The crystal structure and phase composition of the samples were investigated by x-ray diffraction (XRD) with Cu Kα radiation. The microstructure of the sample was observed by transmission electron microscope (TEM). Magnetic measurements were carried out in a Quantum Design physical properties measurement system (Versalab) with a maximum magnetic field of 3 T. All the samples were magnetized under a 10 T pulsed magnetic field before measurement.

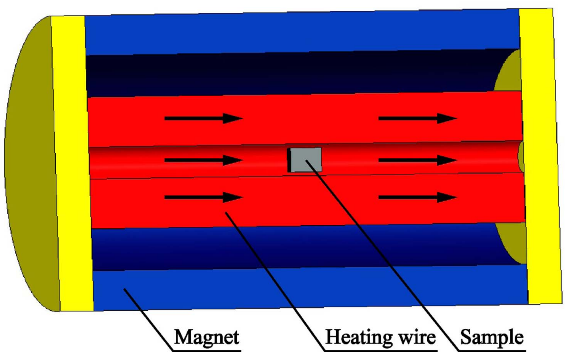

Fig. 1. (Color online) Schematic diagram of magnetic field heat treatment. The blue part represents the permanent magnet, the black arrow represents the direction of the magnetic field, the red part represents the heating body, and the gray part represents the sample.

3. Results and Discussions

Figure 2 shows the XRD patterns of the as-cast $SmCo_5$/α-Fe alloy and the as-milled powders. The XRD results show that there are $SmCo_5$ main phase and a small amount of Sm_2Co_{17} and FeCo phases. For the as-milled powders, the diffraction peaks almost disappear except broadened diffraction peak near 2θ = 45°. It can be concluded that the milled powder consisted of mixture of amorphous phase and crtytalline Fe-Co phase. Figure 3 shows the hysteresis loops of the $SmCo_5$/α-Fe powders after 10 h milling. The coercivity of the as milled

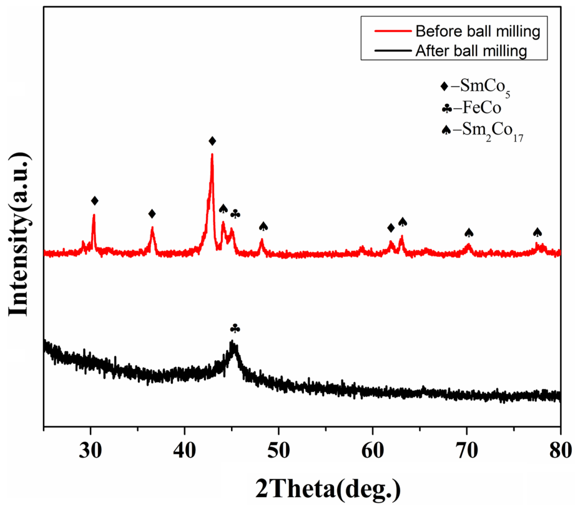

Fig. 2. (Color online) XRD patterns of the as-cast and the as-milled $SmCo_5$/α-Fe powders.

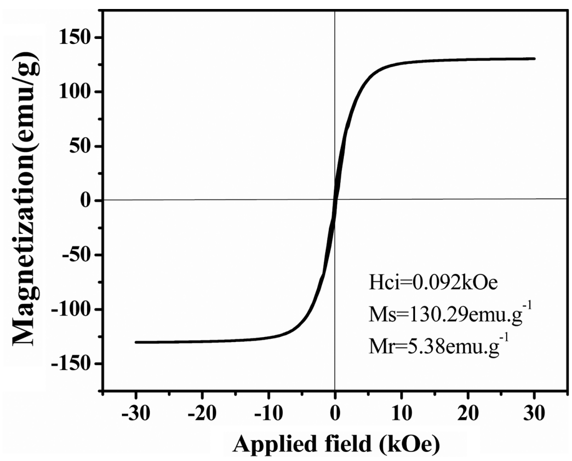

Fig. 3. Hysteresis loops of the as-milled $SmCo_5$/α-Fe powders after 10 h milling.

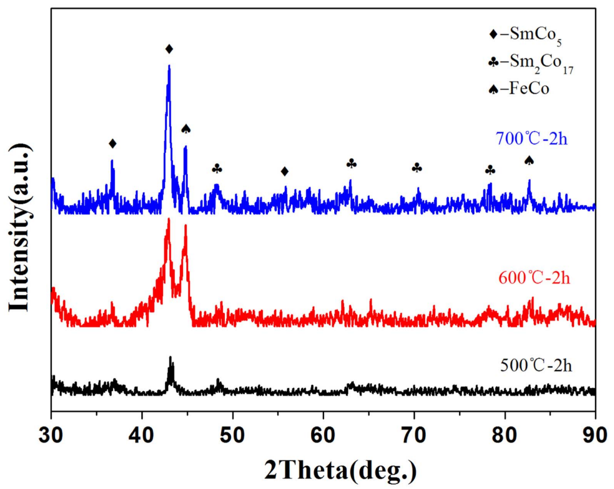

Fig. 4. (Color online) XRD patterns of samples annealed at different temperatures with a magnetic field.

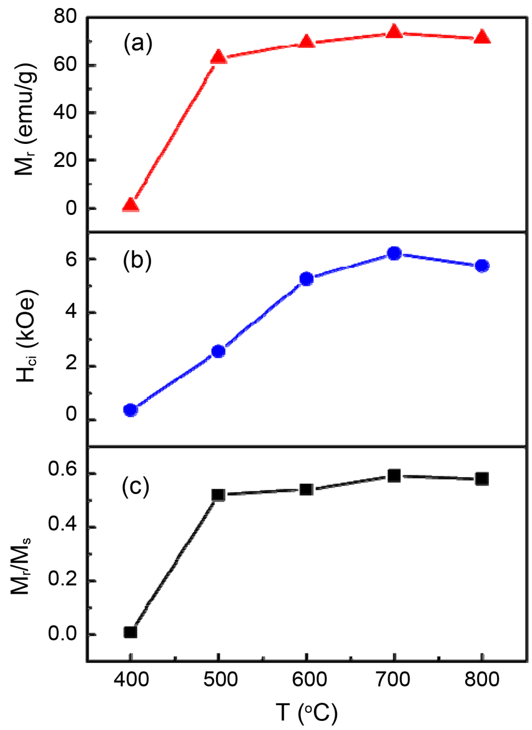

Fig. 5. (Color online) Magnetic properties of the annealed $SmCo_5$/α-Fe samples as a function of annealing temperature with a magnetic field.

powders is only 92 Oe due to the as-milled powders are amorphous state.

Figure 4 shows the XRD patterns of the $SmCo_5$/α-Fe samples after magnetic field annealing at various temperatures for 2 h. It can be seen that the $SmCo_5$ phase is formed at 500 °C. With increasing annealing temperature to 600 °C, the characteristic peaks of the $SmCo_5$ phase are more obvious, and some lower intensity diffraction peaks of Sm_2Co_{17} phase appear. Furthermore, as the annealing temperature reaches 600 °C, the diffraction peaks of FeCo phase appear. Meanwhile, the XRD diffraction peaks are shifted to the right, which may be benefited from the inter-diffusion of the Fe element and Co element leading to form the $Sm(Co, Fe)_5$ phase and FeCo phase (the same phenomenon also shown in Ref. [22]). With annealing temperature rising further to 700 °C, the XRD diffraction peaks become sharp, resulting from the increase of grain size.

Figure 5 shows the magnetic properties of the annealed samples under magnetic field. The sample annealed at 400 °C is still in amorphous state, with low coercivity and remanence. As the annealing temperature rising to 500 °C, the remanence and coercivity increase dramatically to 62.69 emu/g and 2.55 kOe, respectively, indicating that hard magnetic phase grains have been formed from the amorphous alloy, which is consistent with the XRD analysis. With the increase of annealing temperature, the coercivity of the annealed samples increases first, and peaks at 6.20 kOe when the annealing temperature is 700 °C, then decreases slightly to 5.68 kOe at 800 °C, as shown in Fig. 5(a). The remanence in Fig. 5(b) shows the similar variation behavior. When the annealing temperature is 700 °C, the maximum remanence is 73.29 emu/g. In addition, the remanence ratio M_r/M_s is often used to characterize the strength of the exchange coupling. The M_r/M_s is 0.59 at 700 °C, indicating a intergranular exchange coupling in the samples.

Figure 6 shows TEM images of $SmCo_5$/α-Fe samples annealed at 500 °C and 700 °C. For the sample at 500 °C, there are obvious crystalline grains and some amorphous regions, as shown in Fig. 6(a). The grain size of the sample annealed at 500 °C can be estimated to be in the range of 2-6 nm. The corresponding selected area electron diffraction (SAED) result and HRTEM image, with a ring-type characteristic of polycrystalline, reveal a typical $CaCu_5$-type structure, which is good agreement with the corresponding XRD result. For the sample annealed at 700 °C, the TEM and HRTEM images show good crystallization and there is no obvious amorphous region, as shown in Fig. 6(b). The corresponding selected area electron diffraction (SAED) result and HRTEM image, with a ring-type characteristic of polycrystalline, revealing that there are two kinds of grains ($SmCo_5$ and FeCo), which is good agreement with the corresponding XRD result. The grain sizes of both $SmCo_5$ grains and FeCo grains are in the range of 10-20 nm for the sample annealed at 700 °C, which can be estimated from the corresponding TEM and HRTEM images.

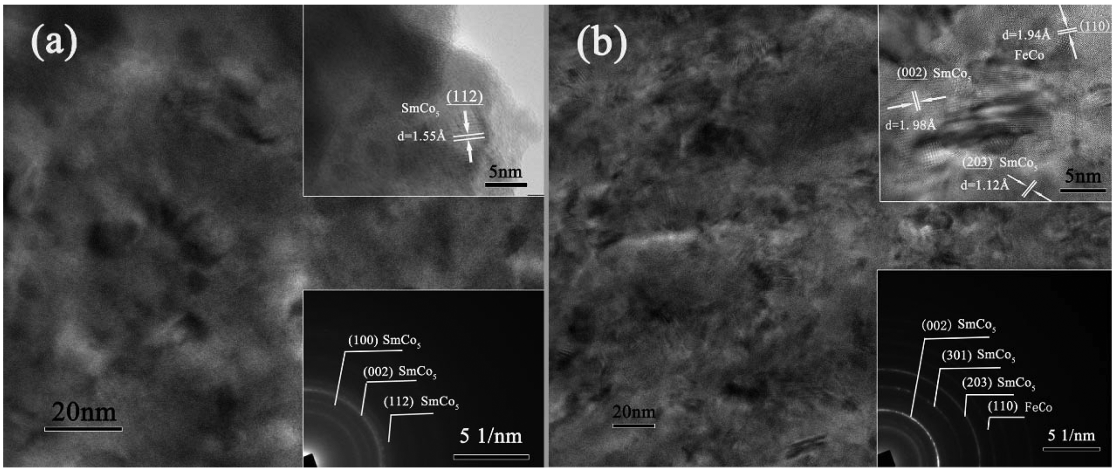

Fig. 6. TEM images and corresponding HRTEM images and SAED patterns (inset) of the SmCo$_5$/α-Fe samples annealed at 500 °C (a) and 700 °C (b) with a magnetic field.

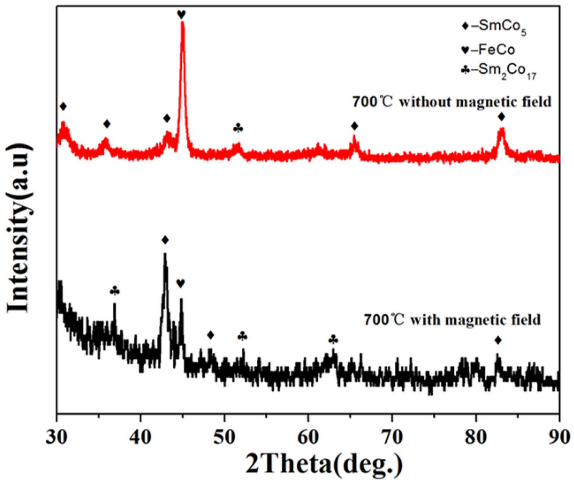

Fig. 7. (Color online) XRD patterns of the SmCo$_5$/α-Fe samples annealed at 700 °C with and without a magnetic field.

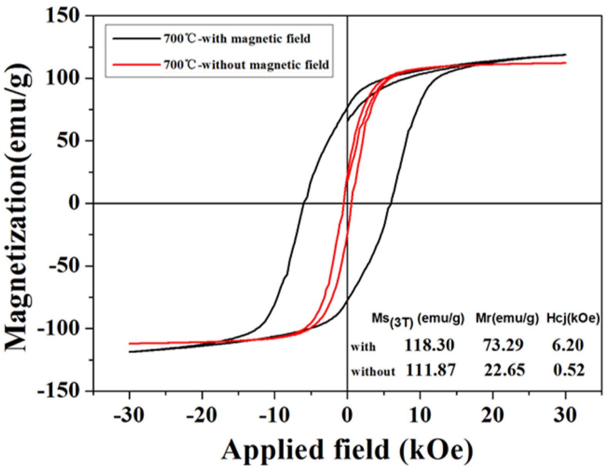

Fig. 8. (Color online) Hysteresis loops of the SmCo$_5$/α-Fe samples annealed at 700 °C with and without a magnetic field.

Figure 7 shows the XRD patterns of the SmCo$_5$/α-Fe samples annealed at 700 °C with and without magnetic field. The diffraction peaks of the SmCo$_5$/α-Fe sample annealed with magnetic field are sharper, indicating better crystalline. The main phases of the samples annealed with magnetic field are FeCo phase and SmCo$_5$ phase. However, the main phase of the samples annealed without magnetic field is only FeCo phase. These results show that the magnetic field during annealing can benefit the crystallization of SmCo$_5$ phase. Meanwhile, the magnetic field could change the transition temperature and induce crystals texture. Due to the lower crystallization temperature than their Curie temperature for Sm-Co phase, the magnetic field plays an important role in the formation of Sm-Co hard magnetic phase during their crystallization process [23-25]. Figure 8 shows the corresponding hysteresis loops and magnetic properties of the SmCo$_5$/α-Fe samples annealed with and without magnetic field. The remanence and coercivity of the SmCo$_5$/α-Fe samples annealed without magnetic field are 23.68 emu/g and 0.52 kOe, respectively. The poor magnetic properties are consistent with the XRD results. For comparison, the remanence and coercivity of the SmCo$_5$/α-Fe samples annealed with the magnetic field are 71.31 emu/g and 5.70 kOe, which are significant higher, suggesting that magnetic field during annealing can help increasing remanence and coercivity, thus optimizing magnetic properties.

4. Summary

Effects of magnetic field heat treatment on the crystallization, microstructure and magnetic properties of the $SmCo_5$/α-Fe nanocomposite permanent magnet were studied. The crystallization temperature, especially for hard $SmCo_5$ phase, can be effectively reduced by applying a magnetic field during the heat treatment for amorphous $SmCo_5$/α-Fe alloy. Thus, magnetic properties can be optimized for good intergranular exchange coupling which is benefit from the good degree of crystallinity of $SmCo_5$/α-Fe alloy. In addition, the magnetic properties of $SmCo_5$/α-Fe magnets can be optimized with the appropriate annealing temperature which can guarantee to acquire both good crystallinity and fine grain size.

Acknowledgement

This work was supported by the Natural Science Foundation of China (51331003) and the International S&T Cooperation Program of China (2015DFG52020).

References

[1] N. Poudyal and J. P. Liu, J. Phys. D. Appl. Phys. **46**, 043001 (2013).
[2] C. B. Rong, Y. Zhang, N. Poudyal, D. P. Wang, M. J. Kramer, and J. P. Liu, J. Appl. Phys. **109**, 07A735 (2011).
[3] C. B. Rong and J. P. Liu, J. Appl. Phys. **105**, 07A714 (2009).
[4] D. W. Hua, M. Yue, J. H. Zuo, R. Pan, D. T. Zhang, W. Q. Liu, J. X. Zhang, Z. H. Guo, and W. Li, J. Alloys Compd. **538**, 173 (2012).
[5] W. Liu, Z. D. Zhang, J. P. Liu, L. J. Chen, L. L. He, Y. Liu, and X. K. Sun, Adv. Mater. **14**, 1832 (2002).
[6] Z. J. Guo, J. S. Jiang, and J. E. Pearson, Appl. Phys. Lett. **81**, 2029 (2002).
[7] J. S. Jiang, J. E. Pearson, and Z. Y. Liu, Appl. Phys. Lett. **85**, 5293 (2004).
[8] Y. Choi, J. S. Jiang, and Y. Ding, Phys. Rev. B **75**, 104432 (2007).
[9] W. B. Cui, Y. K. Takahashi, and K. Hono, Adv. Mater. **24**, 6530 (2012).
[10] V. Neu, S. Sawatzki, M. Kopte, C. Mickel, and L. Schultz, IEEE Trans. Magn. **48**, 3599 (2012).
[11] S. Yang, S. D. Li, X. S. Liu, G. Z. Xie, Z. J. Tian, K. Peng, X. P. Song, and Y. W. Du, The Chinese Journal of Nonferrous Metals. **12**, 1234 (2002).
[12] W. Wang, J. S. Ni, and H. Xu, Journal of the Chinese Society of Rare Earths. **21**, 530 (2003).
[13] X. Q. Bao, S. Z. Zhou, Z. C. Wang, Y. Qiao, and M. C. Zhang, Journal of the Chinese Society of Rare Earths. **21**, 27 (2003).
[14] C. Rong, Y. Zhang, and N. Poudyal, J. Mater. Sci. **46**, 6065 (2011).
[15] W. Q. Liu, J. H. Zuo, and M. Yue, J. Appl. Phys. **109**, 07A741 (2011).
[16] C. Rong, Y. Zhang, and N. Poudyal, Appl. Phys. Lett. **96**, 102513 (2010).
[17] X. H. Li, L. Lou, W. P. Song, G. W. Huang, F. C. Hou, Q. Zhang, H. T. Zhang, J. W. Xiao, B. Wen, and X. Y. Zhang, Adv. Mater. **29**, 1 (2017).
[18] C. J. Yang and E. B. Park, J. Magn. Magn. Mater. **166**, 4428 (2002).
[19] C. Rong, Y. Zhang, N. Poudyal, X. Xiong, M. J. Kramer, and J. P. Liu, Appl. Phys. Lett. **96**, 102513 (2010).
[20] L. X. Lian, Y. Liu, J. Li, and S. J. Gao, The Chinese Journal of Nonferrous Metals. **14**, 2085 (2004).
[21] K. H. J. Buschow and A. S. Van Der Goot, Journal of The Less-Common Metals. **3**, 14 (1968).
[22] Y. Zhang, M. J. Kramer, C. Rong, and J. P. Liu, Appl. Phys. Lett. **97**, 3588 (2010).
[23] J. Y. Zhao, C. J. Li, C. K. Ma, X. F. Ren, Z. Q. Zhang, and Z. M. Ren, J. Alloys Compd. **86**, 631 (2015).
[24] Y. F. Su, H. Su, Y. J. Zhu, F. Wang, J. Du, W. X. Xia, A. R. Yan, J. P. Liu, and J. Zhang, J. Alloys Compd. **375**, 647 (2015).
[25] F. Henrich, H. Rahn, and S. Odenbach, J. Magn. Magn. Mater. **353**, 380 (2015).